Iraqi Journal of Physics, 2018 *Vol.16, No.39, PP. 71-80*

DOI: 10.20723/ijp.16.39.71-80

Characterization of $(SnO_2)_{1-x}(TiO_2:CuO)_x$ films as NH_3 gas sensor

Sara S. Mahmood[1] and Bushra A. Hasan[2]

[1]Ministry of Science and Technology

[2]Department of Physics, College of Science, University of Baghdad

E-mail: sarasadiqphd@gmail.com

Abstract

Tin dioxide (SnO_2) were mixed with (TiO_2 and CuO) with concentration ratio (50, 60, 70, 80 and 90) wt% films deposited on single crystal Si and glass substrates at (523 K) by spray pyrolysis technique from aqueous solutions containing tin (II) dichloride Dihydrate ($SnCl_2$, $2H_2O$), dehydrate copper chloride ($CuCl_2.2H_2O$) and Titanium(III) chloride ($TiCl_3$) with molarities (0.2 M). The results of electrical properties and analysis of gas sensing properties of films are presented in this report. Hall measurement showed that films were n-type converted to p- type as titanium and copper oxide added at (50) % ratio. The D.C conductivity measurements referred that there are two mechanisms responsible about the conductivity, hence it possess two activation energies. Maximum sensitivity 16 % obtained for sample $(SnO_2)_{40}(TiO_2: CuO)_{60}$ toward (NH_3) gas at the operating temperature (473 K), whereas faster response time and recovery time were 20 (s) for (SnO_2) and $(SnO_2)_{20}(TiO_2:CuO)_{80}$ respectively.

Key words

SnO_2 thin films, spray pyrolysis, hall effect, NH_3 gas sensing.

Article info.

Received: Jul. 2018

Accepted: Sep. 2018

Published: Dec. 2018

خواص اغشيه $(SnO_2)_{1-x}$ $(TiO_2: CuO)_x$ كمتحسس لغاز NH_3

ساره صادق محمود[1] و بشرى عباس حسن[2]

[1]وزارة العلوم والتكنولوجيا

[2]قسم الفيزياء، كلية العلوم، جامعة بغداد

الخلاصة

تم تحضير الاغشية الرقيقة من $(SnO_2)_{1-x}$ $(TiO_2: CuO)_x$ وذلك بخلط اوكسيد القصدير مع اوكسيد التيتانيوم و اوكسيد النحاس بنسب وزنية (50, 60, 70, 80 and 90) wt% على قواعد مختلفة مثل الزجاج والسيليكون احادي التبلورباستخدام تقنية الرش الحراري الكيميائي عند درجة حرارة 250 $^{\circ}C$ وذلك بمزج كل من كلوريدي القصدير و النحاس المائي الثنائي وكلوريد التيتانيوم الثلاثي بمولارية (0.2 M). في هذا البحث تم عرض نتائج الخواص الكهربائية وتحليل نتائج التحسس الغازي. اظهرت قياسات تاثير هول ان اغشية اوكسيد القصديركانت نوع سالب التوصيل تتحول الى النوع موجب التوصيل مع مزجها مع كل من اوكسيد التيتانيوم والنحاس عند النسبه (50%). اشارت دراسة التوصيلية المستمرة ان الاغشية لها ميكانيكتا توصيل والذي يعني ان هناك طاقتا تنشيط. اعلى قيمة للتحسسية لغاز (NH_3) كانت 16 % تم الحصول عليها من الغشاء $(SnO_2)_{40}(TiO_2:CuO)_{60}$ عند درجة تشغيل 473 K فيما كان اسرع زمن استجابة وهبوط (s) 20 and 32 لاغشية SnO_2 و $(SnO_2)_{70}(TiO_2:CuO)_{30}$ على التوالي.

Introduction

Many Metal oxide semiconductors (MOS) such as TiO_2,WO_2,In_2O_3, ZnO and SnO_2, have a good detection sensitivity, robustness and the technique is commonly used to monitor a variety of toxic and inflammable gases [1].

When a metal oxide crystal such as SnO_2 is heated at a certain high

temperature in air, oxygen is adsorbed on the crystal surface with a negative charge. Then donor electrons in the crystal surface are transferred to the adsorbed oxygen, resulting in leaving positive charges in a space charge layer. Thus, surface potential is formed to serve as a potential Barrier against electron flow. Inside the sensor, electric current flows through the conjunction parts (grain boundary) of SnO_2 micro crystals. At grain boundaries, adsorbed oxygen forms a potential barrier which prevents carriers from moving freely. The electrical resistance of the sensor is attributed to this potential barrier. In the presence of a deoxidizing gas, the surface density of the negatively charged oxygen decreases, so the barrier height in the grain boundary is reduced, the reduced barrier height decreases sensor resistance [2, 3].

In case of reducing gas, the adsorption of oxygen on the surface extracts conduction electrons from the near surface region forming an electron depleted surface layer, which results in an electric field and a potential barrier associated with this electric field. The potential barrier is depending upon the concentration of adsorbed oxygen. The observed increase and decrease in the sensitivity indicates the adsorption and desorption phenomenon of the gases.

Response of sensors depends on two factors: the speed of chemical reaction on the surface of the grains, and the speed of the diffusion of gas molecules to that surface. At low temperatures the sensor response is restricted by the speed of chemical reactions, and at higher temperature the sensor response is restricted by the speed of the diffusion of gas molecules to that surface. some intermediate temperature the speed values of two processes become equal, and at that point the sensor response reaches its maximum according to this mechanism for every gas there is a specific temperature at which the sensor response attains its peak value [4, 5].

Tin dioxide (SnO_2) is an n-type semiconductor with wide energy band gap (3.7 eV) and have excellent optical and electrical properties. This semiconducting metal oxide is commercially used because of its numerous advantages, including low cost, high chemical stability, high sensitivity to various toxic gases, and compatibility with micro fabrication processes, making them suitable for a wide variety of applications as gas sensors, electrodes in solar cells, infrared reflectors for glass windows, transparent electrodes in electroluminescent lamps and displays etc because of its unique optical, catalytic, and electrical properties [6].

SnO_2 doping can alter its structure and grain size or introduce surface defects. These factors are advantageous for enhancing the gas-sensing responses of SnO_2 toward specific test gases.TiO_2 and CuO mixed SnO_2 exhibit a promising candidate of highly sensitive and selective gas sensors, increased surface area, adsorbed oxygen species, and oxygen vacancy intensity compared with unmixed SnO_2.

Different techniques were adopted to deposit SnO_2 coatings for sensor applications but spray pyrolysis technique routes seem to be the most favoured one due to a simple and low cost-effective processing method and provides uniform and homogeneous layers on various glass substrates. This process enables to control many parameters such us the grain size, the porosity and the thickness of layer [7, 8].

Experimental details

$(SnO_2)_{1-x}(TiO_2{:}CuO)_x$ films were deposited by spray of an aqueous solution including tin (II) dichloride

dihydrate ($SnCl_2$,$2H_2O$), dehydrate copper chloride ($CuCl_2.2H_2O$) and titanium(III) chloride ($TiCl_3$) in 50 ml deionized water and 10 ml of ethanol, onto the preheated glass substrates at temperatures (523K) using compressed air as an atomization gas. The distance between the nozzle and substrate, pressure of the carrier gas, spray time and spray rate were optimized to obtain good-quality $(SnO_2)_{1-x}(TiO_2{:}CuO)_x$ thin films. The substrates were ultrasonically cleaned in acetone and distilled water and dried in air.

The thicknesses (t) can be determined using Optical Interference Fringe Method was calculated by using equation [9]

$$t = \frac{\Delta x}{x} \times \frac{\lambda}{2} \quad (1)$$

Δx: The displacement of the fringe across the film substrate step, x: is the fringe spacing. The structure of prepared thin films was checked by X-ray diffraction (XRD), (Miniflex Model, Rigaku, Japan) using CuKα radiation with a wavelength λ = 1.5418 °A at 2θ values between (20° - 80°).

The crystallite size (D) was calculated using the Scherrer equation as follows:

$$D = 0.9\lambda / FWHM \cos\theta \quad (2)$$

where λ, is the X-ray wavelength, (FWHM) is the Full Width at Half Maximum of the diffraction peak, and Bragg's diffraction angle. The lattice constants (a, b, and c) for of crystal (thin films) can be determined by the equation for tetragonal

$$\frac{1}{d^2} = \frac{(h^2 + k^2)}{a^2} + \frac{l^2}{c^2} \quad (3)$$

where (d) and (hkl) is the inter planar distance and Miller indices, respectively.

Electrical measurements include D.C.-conductivity was calculated using the relation; [10]

$$\sigma_{D.C} = \frac{t}{R.A} \quad (4)$$

where, R: the measured resistance and A : the area of the films in contact with the electrode.

Hall Effect, The values of carrier concentration (n_H), Hall coefficient (R_H), and Hall mobility (μ_H) were calculated using equations:

$$R_H = \frac{V_H}{I}\frac{t}{Bz} \quad (5)$$

V_H: Hall voltage, t: thickness of sample, I_H: constant current, σ: conductivity, and Bz: magnetic field [9].

$$n_H = \frac{1}{R_H.e} \quad (6)$$

where $\mu_H = \sigma.R_H$ (7)

Sensitivity (gas response), selectivity, response time and recovery time are the important characteristics in gas sensing. Selectivity can be defined as the ability of a sensor to respond to a certain gas in the presence of other gases. Response time is defined as the time needed for a sensor to attain 80 % of maximum change in conductance upon the exposure to a test gas, while recovery time as the time taken by a sensor to get back 80 % of the original conductance in air.

The sensor response to reducing gas such as ethanol, methanol, acetone, ammonia, and hydrogen sulphide is detected through the sensors resistance, where the sensitivity is given by [11-13]:

Sensitivity (S)= $\frac{(Rg-Ra)}{Ra}$ If $R_g > R_a$ (8)

Sensitivity (S) = $\frac{(Ra-Rg)}{Ra}$ If $R_a > R_g$ (9)

where, R_g is the change in resistance of the sensor in presence of gas /vapours and R_a is the original resistance of sensor in presence of air.

Results and discussion

Structural characterization

The X ray diffraction spectra of $(SnO_2)_{1-x}(TiO_2{:}CuO)_x$ thin films prepared at (523 K) with different mixing concentration are shown in Fig.1. The diffraction spectra reveals polycrystalline structure for all samples, and the peaks are indexed to JCPDS standard card No. 96-210-4744 [14]. The rutile type phase of SnO_2 with a tetragonal unit cell showing a preferred orientation along (110) plane at ($2\theta = 26.35^o$) that agree with [15].

The peaks of the diffraction are increased by increasing the ratios at (80 and 70) %, then decreasing at (60 and 50) %.

The appearance and disappearance of new peaks as a result of increasing the proportion of mixing and No traces of copper metal or titanium oxides could be detected within the detection limit of XRD, on the other hand there is a slight shift in the major peak of the structure may be attributed to the overlap of (TiO_2 and SnO_2) peaks. In (Table 1) it can be noticed the structural parameters: Angle of diffraction (2θ), the distance between crystal planes (d_{hkl}), Miller indices (hkl), the Full-Width Half Maximum (FWHM) and crystal size (C.S) of films. Indeed the crystal size get to change reach maximum value (25.4) nm at (70 %) SnO_2 concentration which accompanied maximum absorbance as seen later (decreases, increases and return to decrease). Minimum vale (6.1) nm at (60 %) SnO_2 creates favorable conditions for catalytic reactions giving rise to the large surface area and high number of active sites.

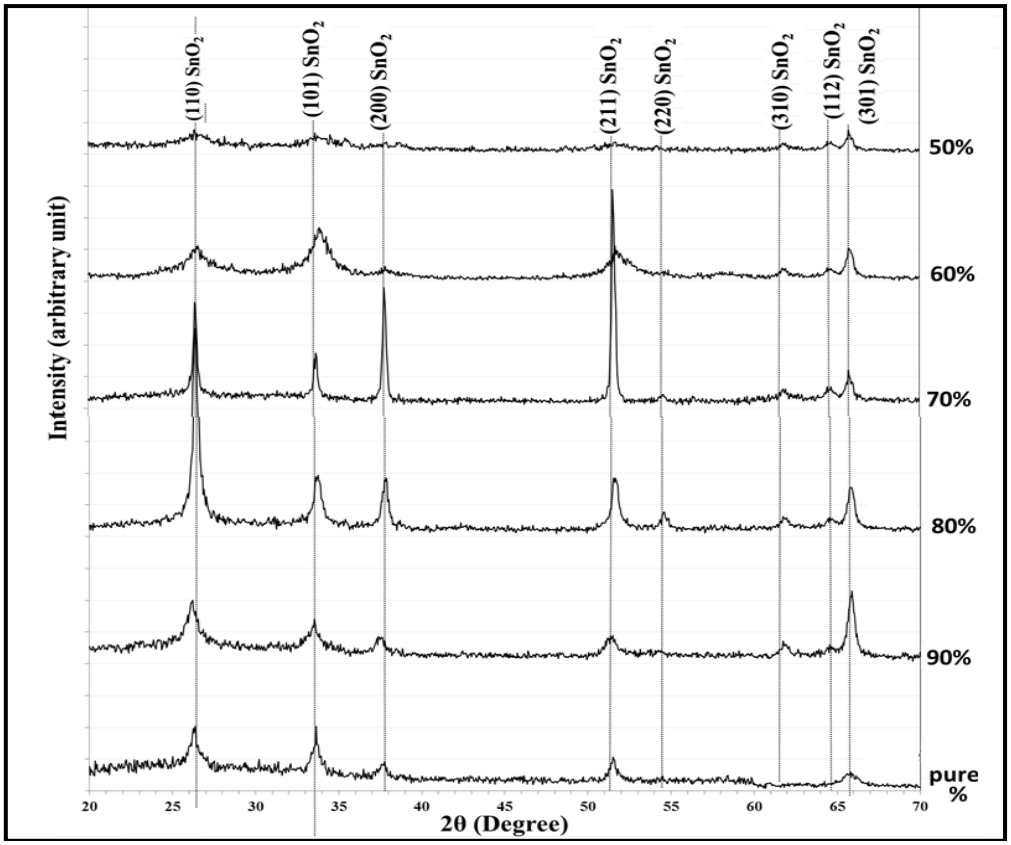

Fig.1:X-ray diffraction patterns of deposited $(SnO_2)_{1-x}$ $(TiO_2{:}\ CuO)_x$ thin films.

Table 1: XRD patterns of $(SnO_2)_{1-x}$ $(TiO_2: CuO)_x$ films with various mixing ratios.

SnO_2%	2θ (Deg.)	FWHM(Deg.)	d_{hkl}Exp.(Å)	C.S (nm)	hkl	d_{hkl}Std.(Å)
Pure	26.3543	0.8344	3.3791	9.8	(110)	3.3498
	33.6714	0.7702	2.6596	10.8	(101)	2.6439
	37.6508	0.6418	2.3872	13.1	(200)	2.3686
	51.5148	0.8344	1.7726	10.6	(211)	1.7642
	65.7638	1.2195	1.4188	7.8	(301)	1.4149
90%	26.2259	0.9627	3.3953	8.5	(110)	3.3498
	33.5430	0.8344	2.6695	9.9	(101)	2.6439
	37.4583	0.7060	2.3990	11.9	(200)	2.3686
	51.4506	0.8344	1.7747	10.6	(211)	1.7642
	61.8485	0.7060	1.4989	13.1	(310)	1.4981
	65.8922	0.5135	1.4164	18.4	(301)	1.4149
80%	26.4185	0.4493	3.3710	18.2	(110)	3.3498
	33.7356	0.6419	2.6547	12.9	(101)	2.6439
	37.8434	0.5134	2.3754	16.4	(200)	2.3686
	51.6431	0.4493	1.7685	19.7	(211)	1.7642
	54.5315	0.5135	1.6814	17.4	(220)	1.6749
	61.8485	0.6419	1.4989	14.4	(310)	1.4981
	64.6085	0.5777	1.4414	16.3	(112)	1.4388
	65.8280	0.7060	1.4176	13.4	(301)	1.4149
70%	26.4185	0.3209	3.3710	25.4	(110)	3.3498
	33.6714	0.3851	2.6596	21.6	(101)	2.6439
	37.7792	0.3210	2.3793	26.2	(200)	2.3686
	51.5789	0.3209	1.7705	27.5	(211)	1.7642
	54.5315	0.5777	1.6814	15.5	(220)	1.6749
	61.8485	0.7060	1.4989	13.1	(310)	1.4981
	64.6727	0.6419	1.4401	14.7	(112)	1.4388
	65.6996	0.5135	1.4201	18.4	(301)	1.4149
60%	26.6110	1.3479	3.3470	6.1	(110)	3.3498
	33.9281	1.0912	2.6401	7.6	(101)	2.6439
	37.8434	0.5776	2.3754	14.5	(200)	2.3686
	51.7073	1.1553	1.7664	7.6	(211)	1.7642
	61.8485	0.7702	1.4989	12.0	(310)	1.4981
	64.6085	0.5777	1.4414	16.3	(112)	1.4388
	65.7638	0.6418	1.4188	14.7	(301)	1.4149
50%	26.2901	1.2195	3.3872	6.7	(110)	3.3498
	33.7356	1.0270	2.6547	8.1	(101)	2.6439
	37.9718	1.1553	2.3677	7.3	(200)	2.3686
	51.5789	1.1553	1.7705	7.6	(211)	1.7642
	61.8485	0.7702	1.4989	12.0	(310)	1.4981
	64.6085	0.6419	1.4414	14.6	(112)	1.4388
	65.7638	0.5776	1.4188	16.4	(301)	1.4149

Hall effect measurements

The Hall Effect measurements checked at room temperature by (Van-der-Pauw) method which is given in Table 2. The charge carrier concentration (n_H), Hall coefficient (R_H) and carrier Hall mobility (μ_H) values were calculated using the

relation (5, 6 and 7). Hall coefficient show that (60, 70, 0, 90 and 100)% of SnO_2 films deposition at (523K) are n-type semiconductors, i.e. Hall voltage decreases with the increase of the current, The negative sign of Hall coefficient indicates that the conductivity nature of the film is n-type, this corresponds to the researcher's findings when preparing the binary compound (SnO_2, TiO_2) [16].

The addition of (CuO and TiO_2) to the host material has different effect on the type of the charge carries, i.e. the sample (50% SnO_2) changed to (p type) semiconductors. The resistivity increases with increasing (Cu, Ti) atoms which suggests that further mixing leads to a substitution of the (Sn^{+4}) ions.

Carrier concentration and mobility values get to change in opposite manner; the increase of charge carriers (reduced of mobility) is attributed to new states in the band gap established by both added oxides.

Table 2: Illustrates carrier concentration (n_H), mobility (μ_H), electrical resistivity(ρ_H), conductivity(σ_H) and hall coefficient (R_H) of $(SnO_2)_{1-X}(TiO_2:CuO)_X$ thin films.

SnO_2%	n_H (cm^{-3})	μ_H (cm^2/vs)	ρ (Ω.cm)	σ_H $(\Omega.cm)^{-1}$	R_H (m^3.C)	type
100(Pure)	-1.92E+14	5.29E+3	1.76E+5	1.67E-3	-3.17E+06	n
90	-1.97E+13	3.54E+2	0.97E+5	0.67E-3	-5.28E+05	n
80	-2.05E+12	1.84E+2	5.21E+4	1.92E-2	-9.58E+03	n
70	-9.94E+10	1.21E+2	1.37E+3	0.64E-2	-1.89E+04	n
60	-7.88E+10	2.23E+0	1.77E+2	7.29E-1	-3.06E+00	n
50	5.02E+11	4.79E+2	2.59E+4	3.86E-3	+1.24E+05	p

D.C. measurements

The resistivity of thin films with different composition ratios was estimated by DC measurements. The samples were heated in the temperature controller oven from room temperature up to 473 K. The resistivity of the films is calculated from the measured electrical resistance. The activation energy is calculated from plotting conductivity (Ln σ) as a function of reciprocal temperature (1/T).

Fig. 2 shows the variation of Ln(σ) with reciprocal temperature for deposited films. From these figures, there are two stages of DC-conductivity mechanism throughout the temperatures range (293-473 K). The first activation energy (Ea_1) occurs at higher temperatures (363-473) K due to conduction of the carrier excited into the extended states beyond the mobility edge. The second activation energy (Ea_2) occurs at low temperatures (298-363) K due to the carriers transport into localized states near the valence or conduction bands [17, 18].

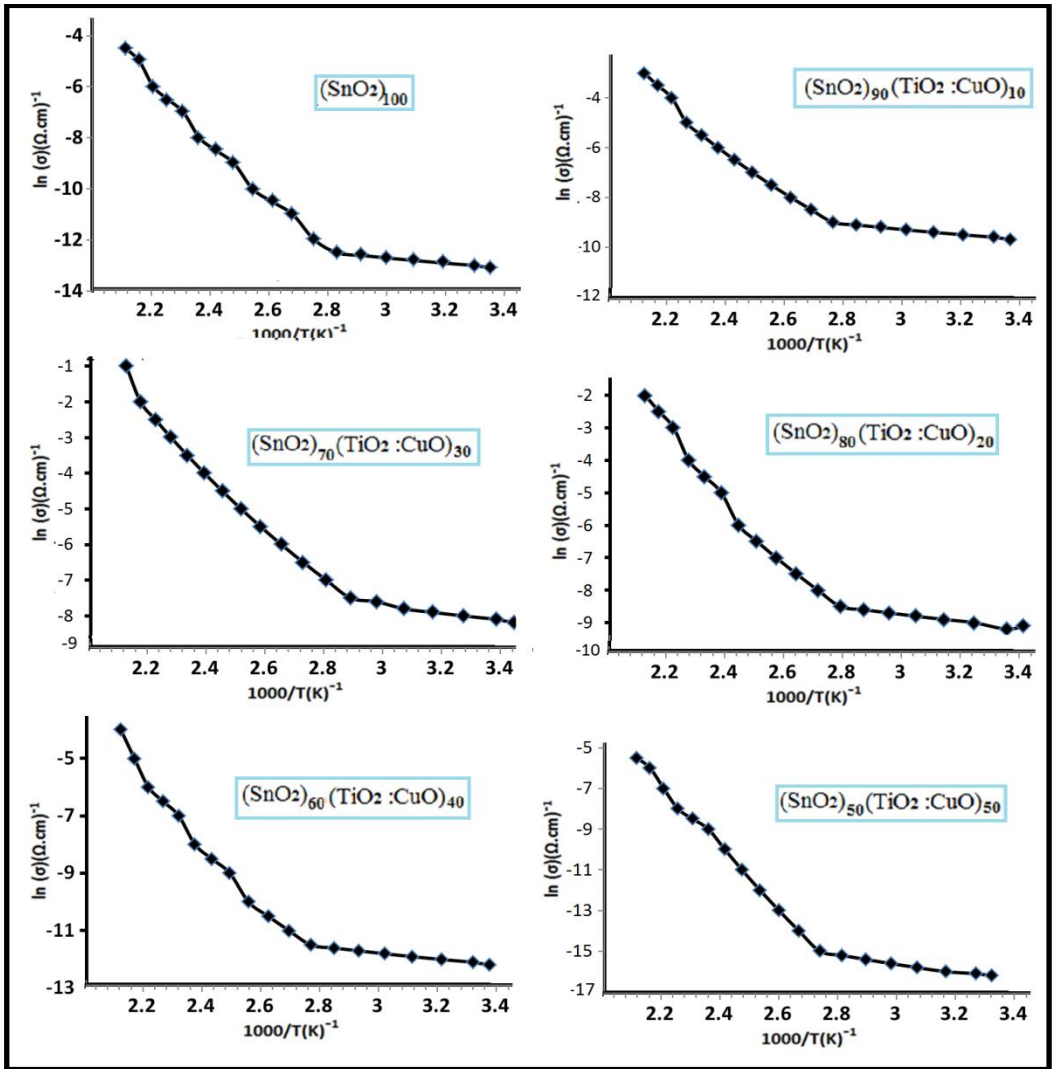

Fig.2: Plot of Ln (σ) vs. 1000/T of $(SnO_2)_{1-X}(TiO_2:CuO)_X$ thin films.

Two activation energies can be observed for pure SnO_2 and (SnO_2:TiO_2:CuO) thin films with different mixing concentration of SnO_2 (90, 80, 70, 60 and 50) wt. % were prepared by (CSP) technique. The activation energy changes in reverse manner to that of conductivity and in the same sequence of energy gap. This result is expected since the activation energy at high temperature range is half the energy gap and can be attributed to the same reasons i.e. the reduction of the activation energy is related to the creation of new states in the band gap which lead to reduction of energy gap while the increment of activation energy is related to the compensation effect of the added dopant as shown in Table 3.

Table 3: D.C activation energies of $(SnO_2)_{1-X}$ $(TiO_2: CuO)_X$ thin films.

SnO_2%	Ea_1 (eV)	Temp. Range(K)	Ea_2 (eV)	Temp. Range(K)	$\sigma_{R.T}$ $(\Omega.cm)^{-1}$
100 (pure)	1.231	353-473	0.163	298-353	7.73E-7
90	0.907	363-473	0.097	298-363	5.12E-3
80	0.899	363-473	0.089	298-363	3.09E-1
70	0.742	363-473	0.112	298-363	3.79E+0
60	0.989	353-473	0.097	298-353	3.58E-3
50	0.994	363-473	0.128	298-363	4.41E-4

Gas sensors

The gas sensitivity of $(SnO_2)_{1-x}(TiO_2{:}CuO)_x$ thin films deposited on to Si(n-type) substrate to NH_3 gas was measured. The sensor's responses to NH_3 gas were recorded at different operating temperature (273, 373, 473 and 573) K. The change in the sensitivity with concentration is small. The sensor sensitivity (S) is proportional to the number of active centres on the surface density of the active centres of sensor.

When such film is heated at higher temperature, oxygen is adsorbed by the tin oxide layer and abstracts electron from the surface states thereby increasing the film resistance. This results in the formation of ionic species such as O^{-2}, O_2^- and O^-. Desorption of these oxygen species at the surface due to the presence of doped atoms would culminate in an increase in conductance of the SnO_2 layer significantly in the presence of the sensing gas (NH_3) gas. Additionally, an increase in conductivity is also due to the reduction of the electronic potential barrier in the grain boundary of SnO_2 when oxygen is adsorbed on its surface. The reactions at the surface of films would be as follows [12, 13 and 15]:

$O_2 + e^- \longrightarrow O^{-2}$

$O_2^- + e^- \longrightarrow 2\,O^-$

Fig. 3 shows the sensitivity to (NH_3) gas as a function of operation temperature for the SnO_2 mixed with different (TiO_2,CuO) concentration. It can be seen that the sensitivity of SnO_2 films change in non-systematic sequence (i.e. increases and decreases) with increasing the (TiO_2, CuO) concentration. It was found that the sample of 40% (TiO_2,CuO) content has the highest sensitivity to (NH_3) gas at operating temperature 473K. Maximum sensitivity is found to corresponded minimum crystal size.

Noteworthy is it well to known that improving the gas-sensing properties demand to prepare very thin sensing layers with high surface-to volume ratio. In the large number of grains which leads to high porosity and large effective surface area available for adsorption of gas species. The gas responsibility tests performed at room temperature showed lowest variation on the film conductivity, the gradual increase in the operating temperature led to an improvement of the films responsibility [19, 20]. The values of Response time, recovery time and sensitivity of pure SnO_2 and mixed with different ratio of (TiO_2, CuO) are shown in Table 4.

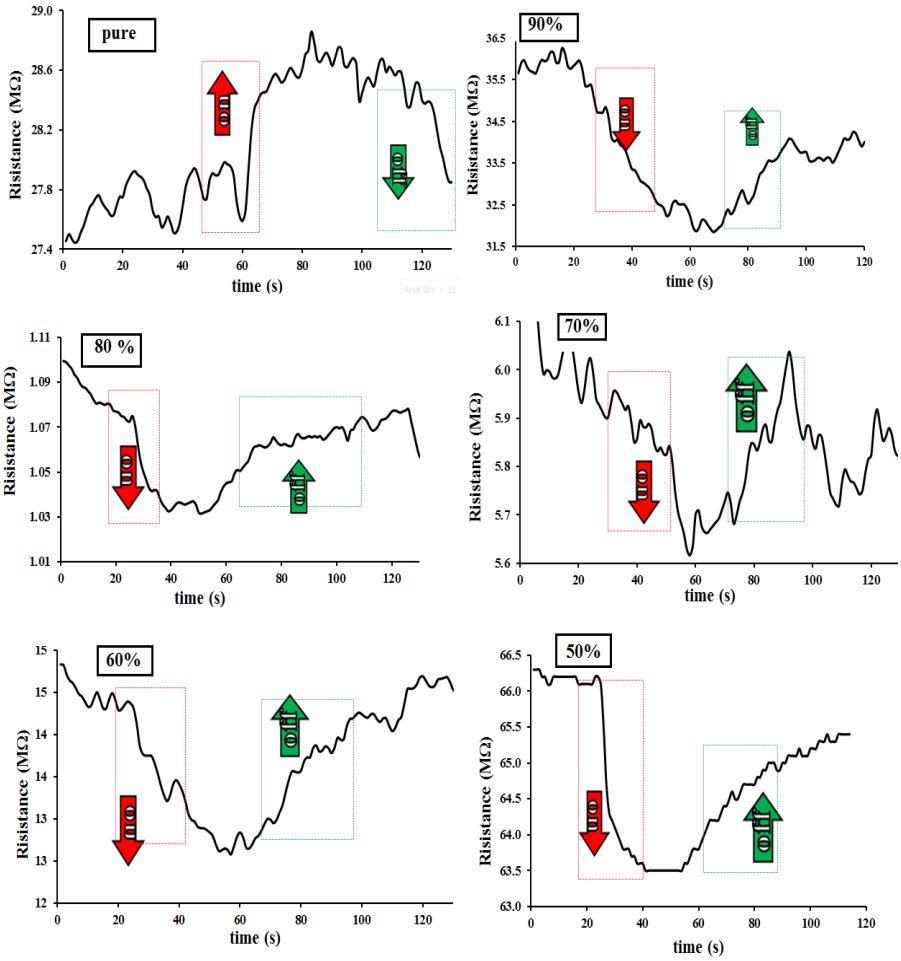

Fig.3: Variation of resistance as a function of $(SnO_2)_{1-x}(TiO_2:CuO)_x$ at operating temperature (473 K).

Table 4: Sensitivity, response and recovery function of operating temperature for $(SnO_2)_{1-x}(TiO_2:CuO)_x$ thin films deposited on n- Si at 473 K.

SnO_2%	Sensitivity (%)	Response time (sec)	recover time (sec)
100	4.3	22	44
90	12.5	50.0	26.0
80	4.9	20.0	38.0
70	7.1	28.0	32.0
60	16.0	34.0	35.0
50	3.9	20	55

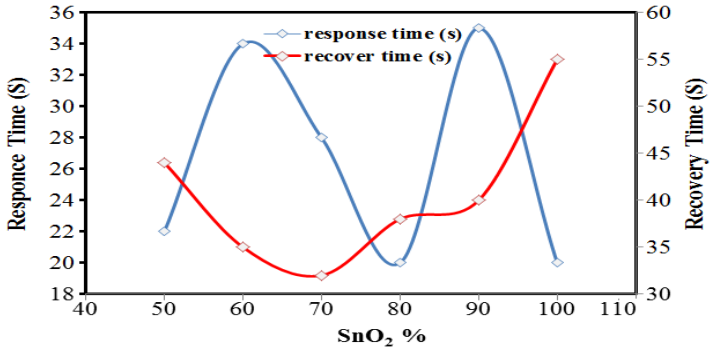

Fig.4: Response and recovery time as function of SnO_2 content for $(SnO_2)_{1-x}(TiO_2:CuO)_x$ thin films deposited on n- Si doped with at 473 K to NH_3 gas.

Conclusions

1- The crystal size increasing of added oxides to the host material decreases.

2-Pure tin oxide and (90, 80, 70 and 60) % SnO_2 is n-type converted to p-type at (50 %)

3- Addition of titanium and copper oxides to SnO_2 creates new states in the band gap, continuous addition will compensates these states.

4- Maximum Sensitivity to NH_3 corresponds to minimum crystal size.

5 -The -$(SnO_2)_{1-x}(TiO_2{:}CuO)_x$ thin film were examined using oxide gas (NO_2) and the results were better than reducing gas sensor.(research under publishing)

References

[1] M. Abdullah, M. Suhail, S. Abbas, Applied Science Research, 4 (2014) 1279-1288.

[2] N. Touidjen, B. Benda Mane, M. Zeggar, F. Mansour, M. Aida, Sensing and Bio-Sensing Research, 11 (2016) 52-57.

[3] O. Fahad, S. Al-Jumaili, M. Suhail, Advances in Environmental Biology, 10 (2016) 89-97.

[4] J. Watson, K. Ihokura G. Coles, Measurement Science and Technology, 4 (1993) 711-719.

[5] M. Boshta, F. Mahmoud, M. Sayed, Journal of Ovonic Research, 6 (2010) 93-98.

[6] S. Roy, A. Bhuiyan, Sensors & Transducers, 195 (2015) 18-24.

[7] E. Ramamurthi, Journal of Optoelectronics and Advanced Materials, 5 (2003) 415-420.

[8] C. Nassiri, A. Hadri, Fz. Chafi, A. El Hat, N. Hassanain, M. Rouchdi, B. Fares, A. Mzerd, JMES, 8 (2017) 420-425.

[9] E. Warren, Addision Wesley Publishing Co.: London (1969).

[10] Y. Singh, Int. J. Mod. Phys., 22 (2013) 745-756.

[11] E. Singha, M. Dharmaprakashb, K. Ramamurthi, Journal of Optoelectronics and Advanced Materials, 6 (2004) 197-203.

[12] S. Sagadevan, J. Podder, Soft Nanoscience Letters, 5 (2015) 55-64.

[13] S. Gadkari, M. Kaur, V. Katti, V. Bhandarkar, K. Muthe, Gupta, Technical Physics & Prototype Engineering Division, (2005) 49-60.

[14] D. Perednis, L. Gauckler, Journal of Electroceramics, 14 (2005)103-111.

[15] F. Ibrahim, "Design and Construction of Low-Pressure D.C.-Sputtering Plasma System for Preparing Gas Sensors", PhD. Thesis, University of Baghdad, Iraq (2013).

[16] M. Sarfi, M. Ghadimi, A. Babaee, Snsor, 1 (2015) 21-26.

[17] M. Batzill, U. Diebold, Prog. Surf. Sci., 79 (2005) 47-54.

[18] A. Gaddari, M. Amjoud, F. Berger, J.B. Sanchez, M. Lahcini, B. Rhouta, D. Mezzane, C. Mavon, MATEC Web of Conferences 5 (2013) 4-10.

[19] A. Yewale, K. Raulkar, S. Wadatkar, T. Lamdhade, Journal of Electron Devices, 11 (2011) 544-550.

[20] Yuan-Chang Liang and Ya-Ju Lo, RSC Adv., 7 (2017) 4724-4734.